IEEE Access
Multidisciplinary | Rapid Review | Open Access Journal

Received 26 July 2022, accepted 28 August 2022, date of publication 5 September 2022, date of current version 15 September 2022.

Digital Object Identifier 10.1109/ACCESS.2022.3204055

RESEARCH ARTICLE

An *In Vitro* Experimental System for 5G 3.5 GHz Exposures

YOUNG SEUNG LEE[1], (Member, IEEE), SANG BONG JEON[1], JEONG-KI PACK[2], NAM KIM[3], AND HYUNG-DO CHOI[1]

[1]Radio and Satellite Research Division, Electronics and Telecommunications Research Institute, Daejeon 34129, South Korea
[2]Department of Radio and Information Communications Engineering, Chungnam National University, Daejeon 34134, South Korea
[3]Department of Computer and Communication Engineering, Chungbuk National University, Cheongju 28644, South Korea

Corresponding author: Young Seung Lee (lys009@etri.re.kr)

This work was supported by the ICT Research and Development Program of MSIT/IITP, a study on public health and safety in a complex EMF environment, under Grant 2019-0-00102.

ABSTRACT In this study, an in vitro experimental system is developed for fifth-generation (5G) 3.5 GHz exposures. A radial transmission line (RTL) housed in an incubator can support the single-mode propagation at a 3.5 GHz band. A conical antenna is also placed at the center of an RTL to ensure field symmetries. A 5G signal generator along with a customized power amplifier can create 5G new radio time division duplex (TDD) waveforms. Additionally, a feedback scheme implemented by employing a directional coupler and power meter allows power control to ensure a steady output power. The system is evaluated based on temperature measurements using the initial temperature slope and nonlinear curve fitting to determine the specific absorption rate (SAR) values. Comparing SARs obtained from a "worst-case" signal of a maximum power condition with the values obtained from a "TDD" signal of an actual 5G TDD transmission gives the initial slope ratio of 0.741, which is very similar to the theoretical duty cycle of 0.743. It is also shown that the average output power, water temperature, incubator air temperature, and CO_2 density are adequately controlled for appropriate in vitro experiments.

INDEX TERMS 5G, *In Vitro*, radial transmission line, 3.5 GHz, TDD.

I. INTRODUCTION

The fifth-generation (5G) communication has recently attracted significant attention worldwide due to the increasing demand for higher data rates and improved capacities. In 2019 [1], South Korea launched the world's first 5G mobile network at a 3.5 GHz band, which is one of the main 5G frequency defined in the 3rd Generation Partnership Project (3GPP) specification as frequency range (FR) 1 [2]. However, few in vitro studies related to 5G exposures have been available despite the worldwide deployment of 5G systems. Therefore, it is essential to develop an in vitro experimental system for 5G exposures to investigate biological and health effects caused by 5G electromagnetic field (EMF). Thus, an in vitro experimental system for 28 GHz, specified in the 3GPP standard as FR2 [2], has been developed in this context [3], [4]. A skin pigmentation effect caused by 28 GHz exposures has also been reported [5].

Various in vitro experimental systems have been available for radio frequency (RF) EMF exposure studies [6]. The open type system of antenna set-ups is usually used for higher frequency bands, such as millimeter-waves [4], [7], [8]. For the closed type, a transverse electromagnetic cell [9], [11], wire patch cell [12], [13], radial transmission line (RTL) [14], [15], [16], and waveguide system [17], [18] have been widely used in most in vitro studies for wireless frequency bands of the previous generations. Since each system has different features for exposures [19], actual types of experiments and cell cultures should be considered for system implementation.

In this study, an in vitro experimental system for 5G 3.5 GHz exposures is developed based on an RTL. Note that this 3.5 GHz spectrum band is the most widely used

The associate editor coordinating the review of this manuscript and approving it for publication was Miguel López-Benítez.

frequency range for 5G commercial networks around the world [20]. The height of an constructed RTL is adjusted compared to the reported ones adopted for in vitro researches of long term evolution (LTE) exposures [21], [22] in order to ensure the single-mode propagation. Moreover, since the required specific absorption rate (SAR) at the cell layer, which is determined by input power characteristics (e.g., stability) of the experimental system, must be well defined [23] in accordance with the safety guideline [19] to conduct reliable exposure experiments, the power control for an amplifier output is also implemented based on a feedback loop to regulate a constant average output power (i.e., an RTL input power). The 5G new radio (NR) time division duplex (TDD) waveforms based on the 3GPP standard [24] are used for temperature measurements to evaluate the SAR values. It can be shown that the SAR of a 5G in vitro experimental system with an arbitrary TDD duty cycle can be assessed based on a downlink-only signal (i.e., a "worst-case" signal as discussed later). The results of real-time control of output power and water temperature are also presented. Additionally, data on long-term monitoring of incubator environmental conditions (air temperature and CO_2) suitable for in vitro cell cultures are shown.

II. MATERIALS AND METHODS

A. SYSTEM DESIGN

Fig. 1 shows a photograph of the entire experimental system. The system consists of an incubator to create a controlled environment for cell cultures, a water circulator to provide temperature cooling to remove thermal effects during exposure, a signal generator to generate a desired 5G signal, and a power amplifier to inject the required power level into an RTL. Note that an RTL for cell exposures and water tray for sustaining an appropriate humidity are housed in an incubator, as shown in Fig. 2. All experimental conditions, such as 5G signal powers, temperature, and CO_2, are continuously monitored using a personal computer (PC) in real-time, as described in Section II-D.

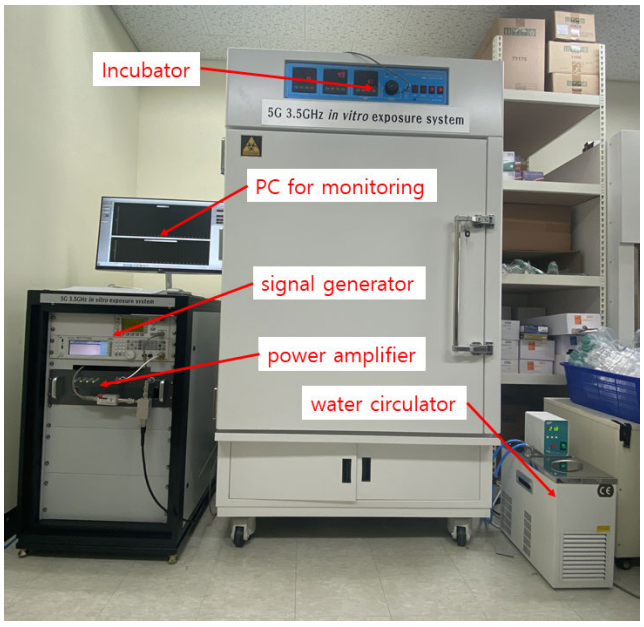

FIGURE 1. Photograph of the entire experimental system for 3.5 GHz In Vitro studies.

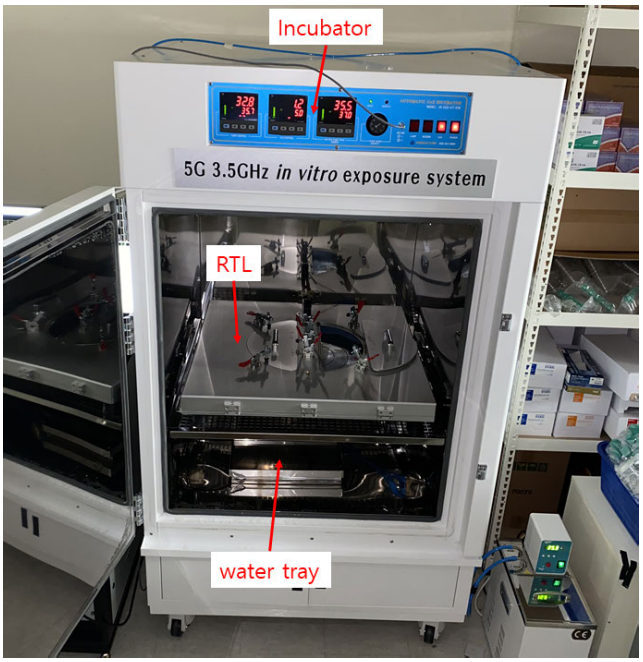

FIGURE 2. RTL and water tray placed in an incubator.

B. RADIAL TRANSMISSION LINE

The 3.5 GHz exposure apparatus designed is based on an RTL. Fig. 3 shows the structural design of an RTL. It is worth noting that the RTL height h is reduced to 35 mm to assure the single-mode propagation inside a waveguide [25], compared to the previous one designed for LTE exposures [22]. The size of 800 mm $\times$ 800 mm allow 12 petri dishes (i.e., six dishes at the inner radius of 100 mm and six dishes at the outer radius of 150 mm) can be placed inside a waveguide. AN-79 broadband flat foam absorbers (Emerson & Cuming) are installed inside the RTL along its outer boundaries to minimize wave reflections. A conical antenna for feeding is installed at the center of the RTL to guarantee azimuthal field symmetries (i.e., to suppress higher-order harmonics using a symmetric antenna) [25]. The feeding gap (i.e., the gap between the antenna and bottom of the RTL) and coupling gap (i.e., the gap between an antenna and ceiling of the RTL) are 1 mm. The apex angle of a conical antenna α is set to 42° based on the minimum reflection loss, as discussed in detail later. The RTL and conical antenna are made of aluminum and gold-plated oxygen-free high conductivity copper, respectively. Additionally, a DRC8 (CPT Inc.) water circulator shown in Fig. 1 is employed to regulate temperatures of the culture medium in petri dishes with the circulating water under the

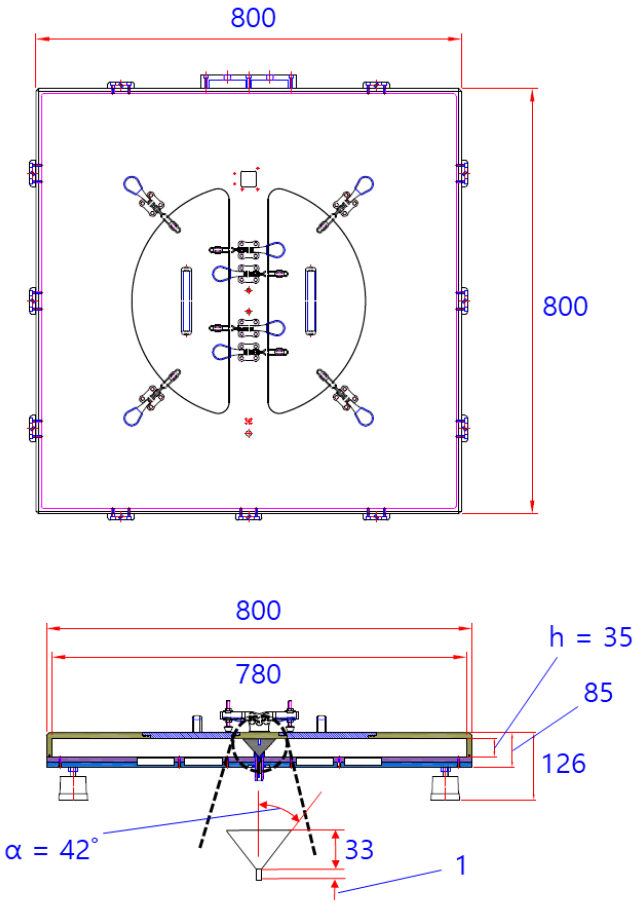

FIGURE 3. Structural design of an RTL (unit: mm).

bottom of the RTL. A cell culture environment inside the RTL can be maintained by introducing an airflow fan for air exchanges from an incubator.

C. 5G EXPOSURE SOURCE

An N5182B signal generator (Keysight Technologies) is employed to provide 5G NR waveforms according to the frame structures defined in the 3GPP standard [24]. Fig. 4 shows the 5G TDD frame structures employed for South Korean mobile operators despite their different carrier frequencies and bandwidths (3.55 GHz and 100 MHz for KT, 3.65 GHz and 100 MHz for SKT, and 3.46 MHz and 80 MHz for LGU+). Note that D, S, U represents the downlink, special, and uplink slot for TDD communications, respectively [26]. It is worth noting that the TDD frame scheme of DDDSU presented in Fig. 4 gives rise to the technology duty cycle of 0.743 [27], [28], which is the scaling factor to determine the time-averaged power considering TDD systems [29]. The 5G signal generated is amplified by a customized power amplifier developed to assure a maximum output power of 150 W. This amplifier output is injected into a conical antenna located at the center of the RTL for exposures. A DC0039A directional coupler (Sungsan)

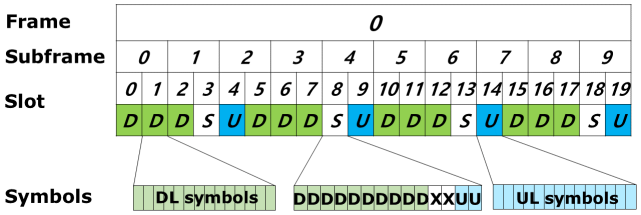

FIGURE 4. 5G TDD frame structures employed for South Korean mobile operators.

and an E4418B power meter (Keysight Technologies) are employed to measure the amplifier output powers. The measured power is used for a feedback loop connected to a 5G signal generator to maintain a constant output power level (i.e., power control). This feedback scheme is implemented to regulate a one-minute average output power, which is crucial to maintain the required SAR values at the cell layer [23] as mentioned earlier.

D. MAIN CONTROL UNIT

A customized software (SW) is developed and installed on a PC to display and monitor measurement results. Fig. 5 shows a schematic of the general configuration of the entire 3.5 GHz in vitro experimental system. During exposure, a PC continuously records all experimental data and controls all feedback flows to regulate desired conditions and settings in real-time. Note that all exposure conditions, e.g., signal level, duration, frequency, and TDD structures can be defined using the main SW. A graphical user interface enables an easy configuration of an experimental setting required. The output power control based on a feedback scheme discussed in II-C is also performed via the SW. All measurement data can be extracted using the SW in a comma-separated values file format as well.

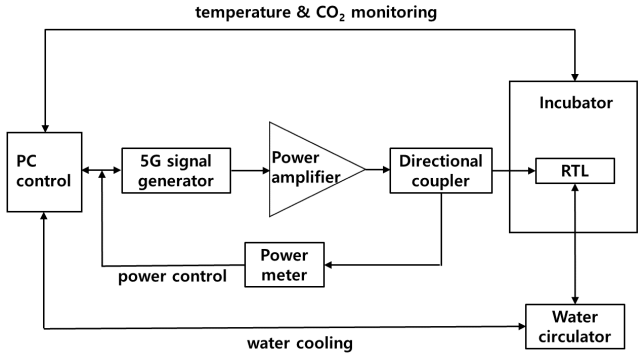

FIGURE 5. Schematic of the general configuration of the entire 3.5 GHz in vitro experimental system.

E. SYSTEM EVALUATION

The developed in vitro experimental system is evaluated based on SAR measurements. Note that the maximum exposure limits at this frequency range of below 6 GHz are expressed in terms of the SAR for whole-body average and

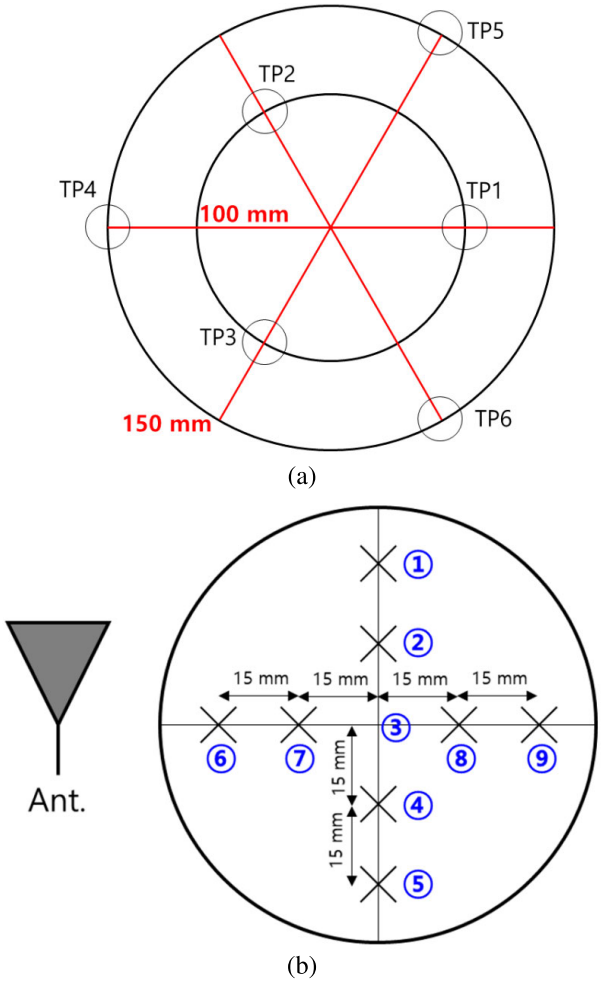

FIGURE 6. **(a) Six positions inside an RTL along two different circumferences; (b) Nine points inside a petri dish for the SAR measurements.**

each body part according to the International Commission on Non-Ionizing Radiation Protection (ICNIRP) guideline [30]. A petri dish with a 90-mm diameter and culture medium with 18-cc volume (about 3-mm medium height) are used for evaluations. Since it is impossible to measure the electric field distribution in the culture medium due to an RTL and field probe structure, i.e., a field probe cannot be inserted in a petri dish during exposures, the SAR evaluation is based on the temperature measurements using a Luxtron 812 two-channel fiber optic thermometer. The temperatures are measured at nine points inside a petri dish located at six different positions inside the RTL along two different circumferences (see Fig. 6). In other words, three positions of TP1 through TP3 and TP4 through TP6 are placed on the circumference of 100 and 150-mm radii, respectively. In each petri dish, points 6 through 9 represent measurements along the radial direction of the RTL, points 1 through 5 are measurements along the perpendicular line, point 6 is the closest point to the antenna, and point 3 denotes the dish center, as depicted in Fig. 6(b). A measurement spacing between points for evaluations are 15 mm. As discussed below, temperatures are recorded in 0.5 s intervals using a thermometer to compute the numerical derivative. Note that all temperature measurements are conducted after a culture medium inside a petri dish reaches room temperature (25 °C) using a water circulator with an incubator door opening to ensure suitable temperature dynamics required for an appropriate curve fitting. Additionally, a testing jig for temperature measurements is designed, as shown in Fig. 7. Small plastic attachments are arranged inside a petri dish to place the thermometer during measurements accurately. Then, SAR can be determined using the following relation

$$\mathrm{SAR} = C \left. \frac{dT}{dt} \right|_{t=0}. \tag{1}$$

Here, C and T are the specific heat and temperature of the culture medium, respectively; t denotes the time during experiments. Therefore, the $\left. \frac{dT}{dt} \right|_{t=0}$ represents the initial temperature slope immediately after the 5G signal is applied. The temperature slope with respect to time is obtained using the nonlinear curve fitting based on the analytical expressions from the one dimensional heat transfer [31].

Two 5G signals are used to measure petri dish SAR. For a "worst-case" signal, all 5G TDD frames in Fig. 4 are used for downlink transmissions. It corresponds to a maximum power condition, i.e., a conservative approach based on the worst-case maximum exposure level. Meanwhile, an actual "TDD" signal consists of uplink-downlink configurations with "DDDSU," as mentioned in Section II-C above. Additionally, the highest amplifier output of 100 W is applied during temperature measurements to achieve a high thermal signal-to-noise ratio [32] to reduce errors caused by numerical derivatives of a noisy function [33]. Then, average SAR in each petri dish position is determined using measured temperatures in nine points shown in Fig. 6(b) using (1) [9], [14].

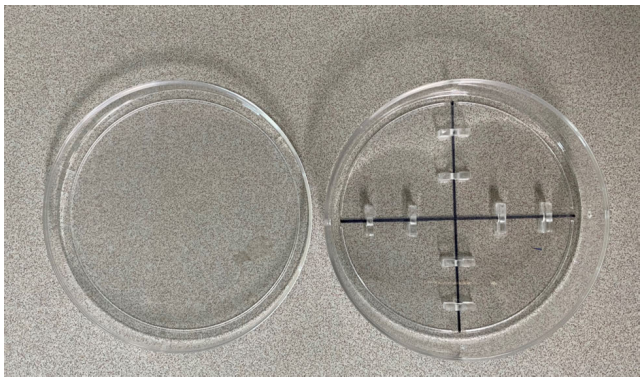

FIGURE 7. **Testing jig for temperature measurements to ensure accurate thermometer placement.**

III. RESULTS AND DISCUSSIONS

A. RTL REFLECTION COEFFICIENT

Prior to actual construction, the optimization of an RTL system is conducted using numerical computations. The simulations and optimizations are performed using the

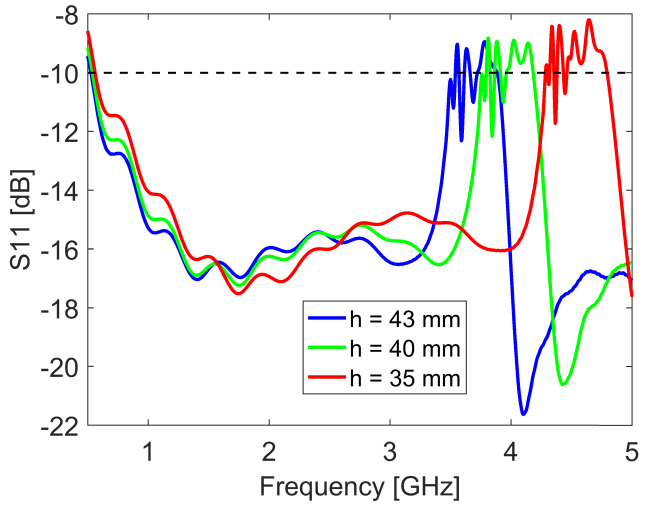

FIGURE 8. Simulated S_{11} at the RTL input port as varying h when $\alpha = 47°$.

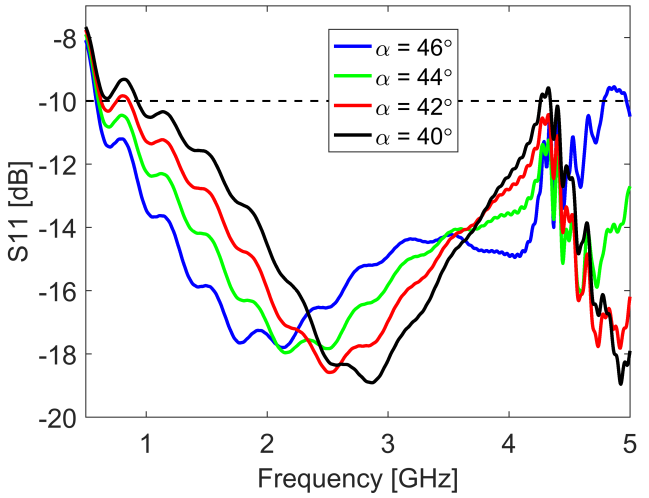

FIGURE 9. Simulated S_{11} at the RTL input port as varying α when $h = 35$ mm.

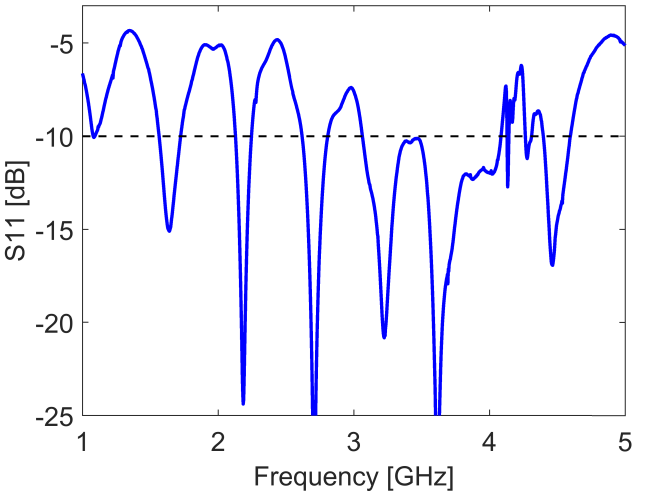

FIGURE 10. Measured S_{11} at the RTL input port when $\alpha = 42°$.

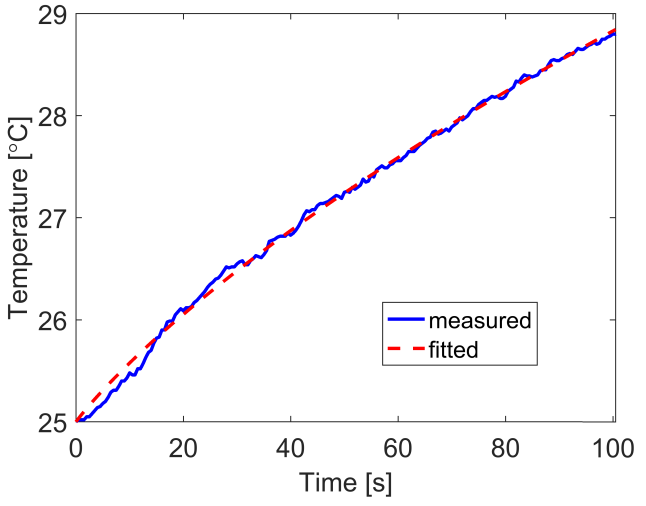

FIGURE 11. Temperature dynamics of a culture medium at the dish center (point 3) on position TP4 for an RTL input power of 100 W with the "worst-case" signal.

electromagnetic simulation software of CST Studio Suite 2021 based on the finite-integration technique (FIT). Based on the relation of the input impedance of a conical antenna $Z_{in} = \frac{\eta}{2\pi} \ln\left[\cot\left(\frac{\alpha}{2}\right)\right]$ [25], $\alpha = 47°$ is used as an initial basis for an optimization to ensure an impedance matching to a 50 Ω line. Fig. 8 presents the simulated reflection coefficient (i.e., S_{11}) at the RTL input port as varying the RTL height h when $\alpha = 47°$. The reason for a larger reflection losses of $S_{11} > -10$ dB at higher frequency band are due to the higher-order mode produced in an RTL with increasing frequency. It can also be observed that this higher-order mode generation is shifted to lower frequency, i.e., the corresponding cutoff frequency increases as the height h decreases. Fig. 9 shows the simulated reflection coefficient (i.e., S_{11}) at the RTL input port as varying the antenna apex angle α when $h = 35$ mm. Broadband characteristics of the RTL can be clearly seen. Additionally, good solution candidates of an optimal apex angle to provide appropriate matching across 5G 3.5 GHz spectrum bands can be $\alpha = 46°$, 44°, and 42°. Fig. 10 shows the measured S_{11} profiles when $\alpha = 42°$, which achieves the best S_{11} characteristic among three candidates during actual measurements for constructions. An E5272A (Agilent) vector network analyzer is used for S_{11} measurements. It can be seen that a reasonable reflection characteristic across 3.5 GHz bands can be achieved for 5G exposure experiments.

B. SAR DOSIMETRY

Fig. 11 shows the temperature dynamics of a culture medium measured at the dish center (i.e., point 3) on test position TP4 in Fig. 6 for an RTL input power P_{in} of 100 W (i.e., an amplifier output power of 100 W). A fitted temperature profile based on the analytical model is also shown. Note that the "worst-case" signal explained in Section II-E is used for

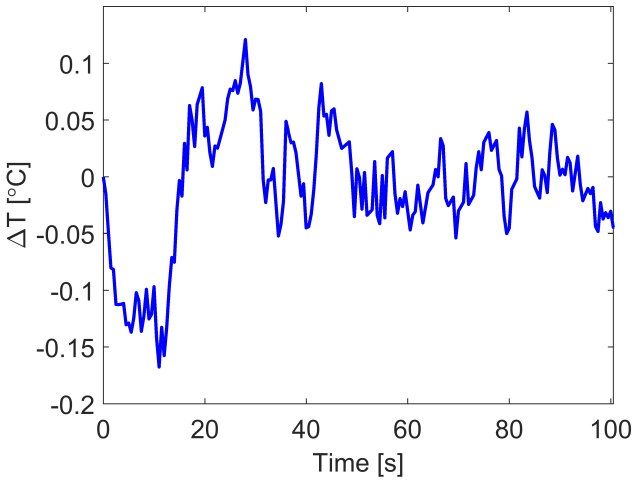

FIGURE 12. Temperature difference ΔT of a culture medium at the dish center (point 3) on position TP4 with the "worst-case" signal.

TABLE 1. Computed SARs normalized to 1 W and RTL input powers P_{in} required for 1 W/kg SAR over nine measurement points on position TP4 with the "worst-case" signal.

Points	Initial slope [°C/s]	SAR per Watt [(W/kg)/W]	P_{in} for 1 W/kg [W]
1	0.03983	1.53	0.654
2	0.05879	2.26	0.443
3	0.06974	2.68	0.373
4	0.07187	2.76	0.362
5	0.04877	1.87	0.534
6	0.04734	1.82	0.550
7	0.04794	1.84	0.543
8	0.04682	1.80	0.556
9	0.15198	5.84	0.171
Average	0.07434	2.86	0.350

TABLE 2. Computed average SARs normalized to 1 W and RTL input powers P_{in} required for 1 W/kg SAR over the inner and outer circumferences with the "worst-case" signal.

Radius [mm]	Initial slope [°C/s]	SAR per Watt [(W/kg)/W]	P_{in} for 1 W/kg [W]
100 (Inner)	0.08004	3.07	0.325
150 (Outer)	0.06679	2.57	0.390

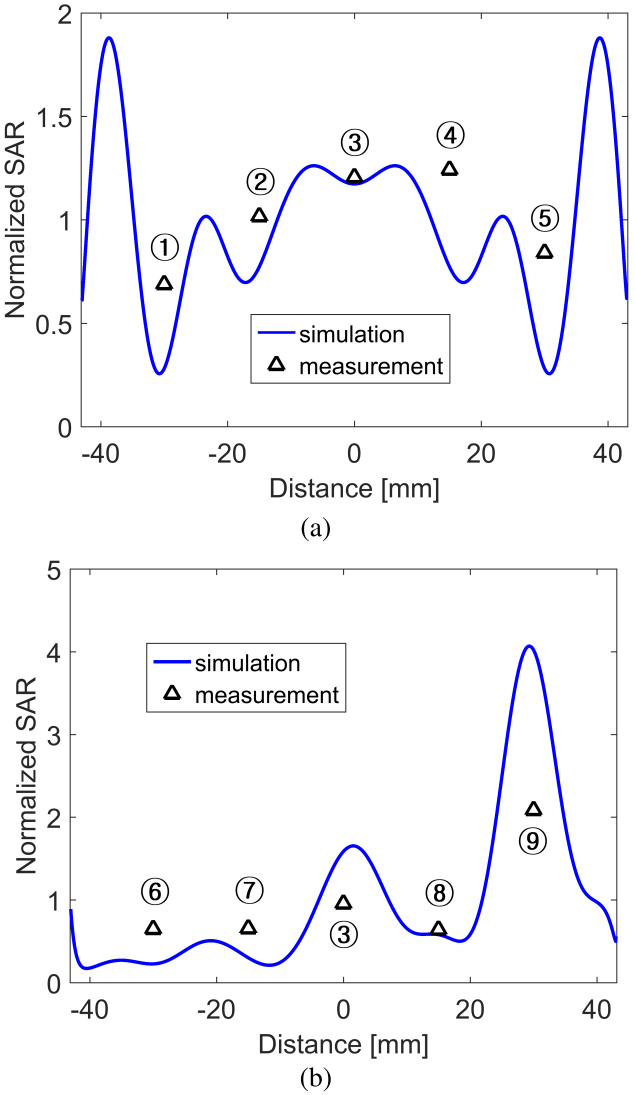

FIGURE 13. Simulated and measured SAR profiles; (a) along the transverse axis; (b) along the longitudinal axis.

measurements. Temperature noise from measurements can be filtered out through a nonlinear curve fitting, permitting a reasonable computation of the initial temperature slope. Fig. 12 shows a temperature difference ΔT between the measured and fitted profiles at the same position. A fairly good agreement between two temperature profiles can be clearly seen and quantified by about $|\Delta T_{\max}| < 0.2$°C. Table 1 summarizes the computed SARs normalized to 1 W RTL input power based on the temperature slope determined and required input powers P_{in} for the 1 W/kg SAR over nine measurement points on position TP4. Higher SAR exposure levels required to study 5G EMF health concerns can be fully achieved, which is about 50 times larger than the basic restrictions for the general public specified in the ICNIRP guideline [30]. The simulated and measured SAR values are compared to confirm these measurement results. Note that the SAR simulations are conducted using the CST Studio Suite 2021, which is the same as that used in S_{11} simulations (see Section III-A). Simulated results are obtained at the height of 1.5 mm from the bottom of a petri dish (i.e., the average height of an 8-cc culture medium) along the transverse and longitudinal axes, corresponding to a line passing through measurement points 1 to 5 and 6 to 9 in Fig. 6(b), respectively. Fig. 13 shows both SAR profiles, which are normalized to their respective average SAR for comparison. Despite some differences due to the uncertainties, overall tendencies are consistent.

Fig. 14 shows the long-term temperature dynamics for two different 5G signals of "worst-case" and "TDD" at

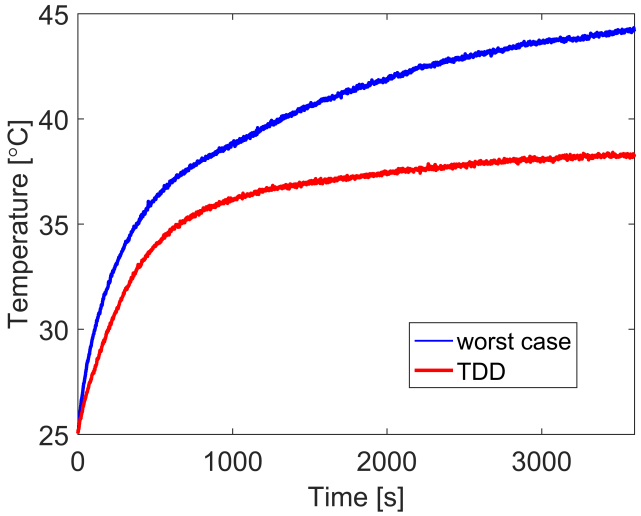

FIGURE 14. Long-term temperature dynamics for two different 5G signals at the dish center (point 3) on position TP4.

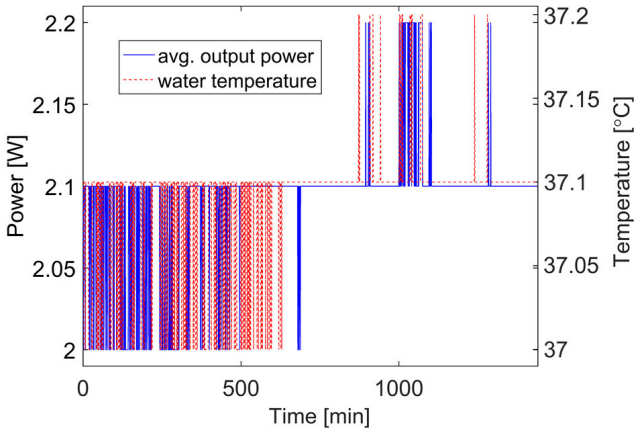

FIGURE 15. Stability of an average output power and water temperature.

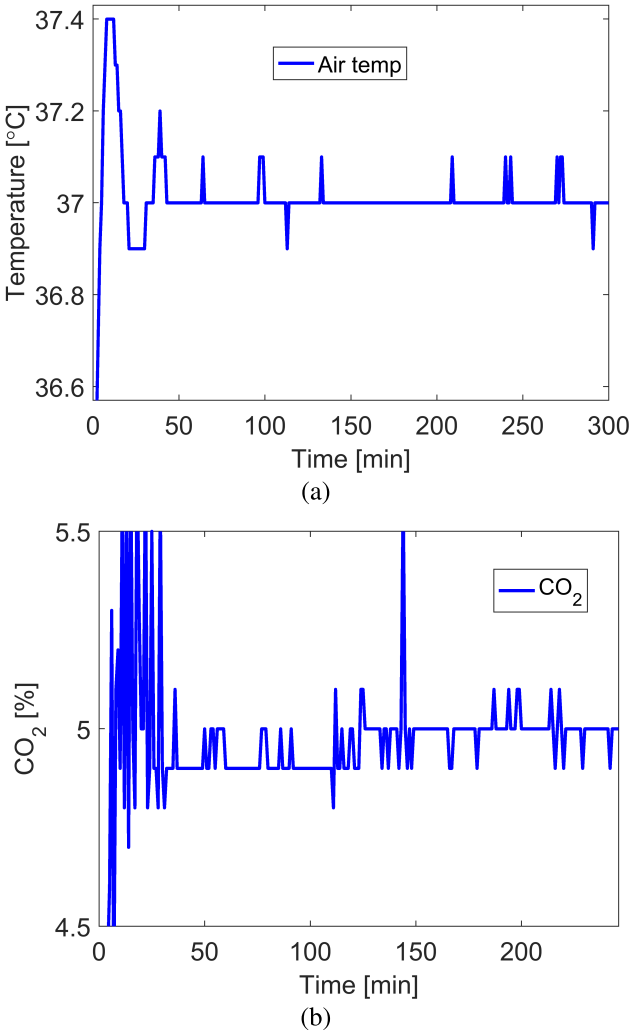

FIGURE 16. Long-term evaluation of an incubator environmental control; (a) an air temperature; (b) a CO_2 density.

the dish center (point 3) on position TP4. Higher temperature rise and corresponding initial slope can be seen with the "worst-case" signal. This result is consistent with the thermal transient phenomenon presented in [34], which is based on the analytical heat transfer and pulse waveforms of the global system for mobile communications along with the time-averaged power. Furthermore, the initial temperature slopes computed are 0.06479 and 0.04799 for the "worst-case" and "TDD" signal, respectively, corresponding to the ratio of 0.741, which agrees closely with the theoretical factor of 0.743 stated in Section II-C. These suggest that the SAR of an experimental system for 5G exposures with an input signal possessing an arbitrary TDD technology duty cycle can be assessed based on temperature measurements using a "worst-case" signal and the corresponding theoretical duty cycle factor. Table 2 presents the average SARs normalized to 1 W and required P_{in} for the 1 W/kg SAR with the "worst-case" signal evaluated over the inner and outer circumferences, i.e., the radii of 100 and 150 mm in Fig. 6(a). In other words, SARs are averaged over TP1 through TP3 and TP4 through TP6 for the inner and outer circumferences, respectively. Using the results presented in Table 2 and the theoretical factor of 0.743, the average SARs normalized to 1 W with the "TDD" signal can be obtained as 2.28 and 1.91 (W/kg)/W over the inner and outer circumferences, respectively. Therefore, the relationship can be derived for the property of an RTL input power P_{in} to obtain a given SAR value as follows:

$$P_{in}|_{inner\ radius}\ [\mathrm{W}] = 0.438 \times SAR\ [\mathrm{W/kg}], \quad (2)$$

$$P_{in}|_{outer\ radius}\ [\mathrm{W}] = 0.525 \times SAR\ [\mathrm{W/kg}]. \quad (3)$$

Therefore, different input powers P_{in} should be applied according to (2) and (3) to different dish positions during experiments, even though target exposure SAR levels are identical.

C. ENVIRONMENTAL CONTROL

Fig. 15 shows the stability of a one-minute average amplifier output power (see Section II-C) and a water temperature used for a water circulation (see Section II-B). The power

fluctuation has a relative standard deviation (RSD) of 1.79%, indicating that an average output power can be maintained within an RSD of the maximum of 3% at worst over a longer period of time. It is also confirmed that a water temperature, which is quite similar to that of a culture medium temperature inside a petri dish, is maintained within ±0.1 °C around 37.1 °C. A small difference from the stated goal of 37 °C can be attributed to an RTL air condition and the accuracy of a thermometer. However, it can easily be compensated by applying an offset value.

Additionally, a long-term evaluation of an incubator environmental control is performed. An incubator air temperature requires about 50 min to reach a steady-state, as shown in Fig. 16(a). Small temperature fluctuations of less than 0.1 °C around 37 °C is also seen after a steady-state. Fig. 16(b) shows a CO_2 density inside an incubator. The results show that the final CO_2 density after 150 min to approach a steady-state is stable within the range of 0.1 %, which is appropriate for cell cultures during 5G exposure experiments.

IV. CONCLUSION

In this study, an in vitro experimental system for 5G 3.5 GHz exposures is developed based on an RTL. A conical antenna is placed at the center of an RTL to ensure field symmetries over petri dish positions. The apex angle α of an antenna is selected based on the optimization to minimize the reflection loss. The measured S_{11} results show that an implemented RTL can be suitable for 5G exposures across a 3.5 GHz band. The power control is also implement to maintain an average output power of an amplifier in order to provide the accurate SAR values. Additionally, two 5G NR TDD waveforms based on the 3GPP frame structures, a ''worst-case'' signal for maximum power and a ''TDD'' signal for practical 5G TDD configurations, are used for actual temperature measurements to evaluate SAR of an in vitro experimental system. The two measured SARs obtained with the nonlinear curve fitting achieve a ratio of 0.741, which is consistent with the theoretical duty cycle of 0.743. This indicates that an experimental system for 5G exposures can be evaluated based on temperature SAR measurements using a maximum ''worst-case'' signal with the corresponding theoretical duty cycle of a TDD transmission considered. Overall trends of the measurement and simulation results also have a good agreement. An average output power, water temperature, incubator air temperature, and CO_2 density are also well controlled for reasonable in vitro 5G experiments. Using an in vitro experimental system developed, actual 3.5 GHz exposures will be performed to investigate the possible health effects of 5G EMF.

ACKNOWLEDGMENT

The authors would like to thank Eretec Inc. for their support and assistance with this article. (Young Seung Lee and Sang Bong Jeon contributed equally to this work.)

REFERENCES

[1] *Reuters. S. Korea First to Roll Out 5G Services, Beating U.S. and China*. Accessed: Jul. 22, 2022. [Online]. Available: https://www.reuters.com/article/southkorea-5g/skorea-first-to-roll-out-5g-services-beating-us-and-china-idUSL3N21K114

[2] *NR Base Station Radio Transmission and Reception*, Standard 3GPP TS 38.104 V 17.5.0, Mar. 2022.

[3] Y. S. Lee, J. Chung, S. B. Jeon, A. Lee, and H. Choi, ''Proposal of 28 GHz *in vitro* exposure system based on field uniformity for three-dimensional cell culture experiments,'' *Bioelectromagnetics*, vol. 40, no. 7, pp. 445–457, Aug. 2019.

[4] Y. S. Lee, P. A. Dzagbletey, J. Chung, S. B. Jeon, A. Lee, N. Kim, S. J. Song, and H. Choi, ''Implementation of an *in vitro* exposure system for 28 GHz,'' *ETRI J.*, vol. 42, no. 6, pp. 837–845, Dec. 2020.

[5] K. Kim, Y. S. Lee, N. Kim, H.-D. Choi, D.-J. Kang, H. R. Kim, and K.-M. Lim, ''Effects of electromagnetic waves with LTE and 5G bandwidth on the skin pigmentation *in vitro*,'' *Int. J. Mol. Sci.*, vol. 22, no. 1, p. 170, Dec. 2020.

[6] J. W. Hansen, E. M. Swartz, J. D. Cleveland, S. M. Asif, B. Brooks, B. D. Braaten, and D. L. Ewert, ''A systematic review of *in vitro* and *in vivo* radio frequency exposure methods,'' *IEEE Rev. Biomed. Eng.*, vol. 13, pp. 340–351, Apr. 2020.

[7] M. Zhadobov, C. N. Nicolaz, R. Sauleau, F. Desmots, D. Thouroude, D. Michel, and Y. L. Dréan, ''Evaluation of the potential biological effects of the 60-GHz millimeter waves upon human cells,'' *IEEE Trans. Antennas Propag.*, vol. 57, no. 10, pp. 2949–2956, Oct. 2009.

[8] S. Koyama, E. Narita, Y. Suzuki, T. Shiina, M. Taki, N. Shinohara, and J. Miyakoshi, ''Long-term exposure to a 40-GHz electromagnetic field does not affect genotoxicity or heat shock protein expression in HCE-T or SRA01/04 cells,'' *J. Radiat. Res.*, vol. 60, no. 4, pp. 417–423, Jul. 2019.

[9] N. Nikoloski, J. Fröhlich, T. Samaras, J. Schuderer, and N. Kuster, ''Reevaluation and improved design of the TEM cell *in vitro* exposure unit for replication studies,'' *Bioelectromagnetics*, vol. 26, no. 3, pp. 215–224, Apr. 2005.

[10] J.-Y. Kim, S.-Y. Hong, Y.-M. Lee, S.-A. Yu, W. S. Koh, J.-R. Hong, T. Son, S.-K. Chang, and M. Lee, ''*In vitro* assessment of clastogenicity of mobile-phone radiation (835 MHz) using the alkaline comet assay and chromosomal aberration test,'' *Environ. Toxicol.*, vol. 23, no. 3, pp. 319–327, Jun. 2008.

[11] G. Del Vecchio, A. Giuliani, M. Fernandez, P. Mesirca, F. Bersani, R. Pinto, L. Ardoino, G. A. Lovisolo, L. Giardino, and L. Calzà, ''Effect of radiofrequency electromagnetic field exposure on *in vitro* models of neurodegenerative disease,'' *Bioelectromagnetics*, vol. 30, no. 7, pp. 564–572, Oct. 2009.

[12] L. Laval, P. Leveque, and B. Jecko, ''A new *in vitro* exposure device for the mobile frequency of 900 MHz,'' *Bioelectromagnetics*, vol. 21, no. 4, pp. 255–263, May 2000.

[13] L. Ardoino, ''1800 MHz *in vitro* exposure device for experimental studies on the effects of mobile communication systems,'' *Radiat. Protection Dosimetry*, vol. 112, no. 3, pp. 419–428, Nov. 2004.

[14] E. G. Moros, W. L. Straube, and W. F. Pickard, ''The radial transmission line as a broad-band shielded exposure system for microwave irradiation of large numbers of culture flasks,'' *Bioelectromagnetics*, vol. 20, no. 2, pp. 65–80, 1999.

[15] W. F. Pickard, W. L. Straube, and E. G. Moros, ''Experimental and numerical determination of SAR distributions within culture flasks in a dielectric loaded radial transmission line,'' *IEEE Trans. Biomed. Eng.*, vol. 47, no. 2, pp. 202–208, Feb. 2000.

[16] K.-Y. Lee, B. C. Kim, N.-K. Han, Y.-S. Lee, T. Kim, J.-H. Yun, N. Kim, J.-K. Pack, and J.-S. Lee, ''Effects of combined radiofrequency radiation exposure on the cell cycle and its regulatory proteins,'' *Bioelectromagnetics*, vol. 32, no. 3, pp. 169–178, Apr. 2011.

[17] J. Schuderer, D. Spat, T. Samaras, W. Oesch, and N. Kuster, ''*In vitro* exposure systems for RF exposures at 900 MHz,'' *IEEE Trans. Microw. Theory Techn.*, vol. 52, no. 8, pp. 2067–2075, Aug. 2004.

[18] A. Schirmacher, S. Winters, S. Fischer, J. Goeke, H.-J. Galla, U. Kullnick, E. B. Ringelstein, and F. Stögbauer, ''Electromagnetic fields (1.8 GHz) increase the permeability to sucrose of the blood-brain barrier *in vitro*,'' *Bioelectromagnetics*, vol. 21, no. 5, pp. 338–345, Jul. 2000.

[19] F. Schönborn, K. Poković, M. Burkhardt, and N. Kuster, ''Basis for optimization of *in vitro* exposure apparatus for health hazard evaluations of mobile communications,'' *Bioelectromagnetics*, vol. 22, no. 8, pp. 547–559, Nov. 2001.

[20] M. M. Blue, S. Yrjola, V. seppanen, P. Ahokangas, H. Hammainen, and M. L. Aho, "Analysis of spectrum valuation elements for local 5G networks: Case study of 3.5-GHz band," *IEEE Trans. Cogn. Commun. Netw.*, vol. 5, no. 3, pp. 741–753, Sep. 2019.
[21] J. Choi, K. Min, S. Jeon, N. Kim, J.-K. Pack, and K. Song, "Continuous exposure to 1.7 GHz LTE electromagnetic fields increases intracellular reactive oxygen species to decrease human cell proliferation and induce senescence," *Sci. Rep.*, vol. 10, no. 1, p. 9238, Jun. 2020.
[22] K. Yoon, S. Choi, H.-D. Choi, N. Kim, S. B. Jeon, K.-M. Lim, H.-J. Lee, and Y.-S. Lee, "Effects of radiofrequency electromagnetic fields and ionizing radiation on amyloid precursor protein processing and cell death," *J. Electromagn. Eng. Sci.*, vol. 20, no. 4, pp. 307–319, Oct. 2020.
[23] N. Kuster and F. Schonborn, "Recommended minimal requirements and development guidelines for exposure setups of bio-experiments addressing the health risk concern of wireless communications," *Bioelectromagnetics*, vol. 21, no. 7, pp. 508–514, Oct. 2000.
[24] *NR Physical Layer Procedures for Control*, Standard 3GPP TS 38.213 V 17.1.0, Mar. 2022.
[25] C. A. Balanis, *Advanced Engineering Electromagnetics*. Hoboken, NJ, USA: Wiley, 1989.
[26] D. Franci, S. Coltellacci, E. Grillo, S. Pavoncello, T. Aureli, R. Cintoli, and M. D. Migliore, "An experimental investigation on the impact of duplexing and beamforming techniques in field measurements of 5G signals," *Electronics*, vol. 9, no. 2, p. 223, Jan. 2020.
[27] S. Jeon, A.-K. Lee, J. Um, and H.-D. Choi, "Estimation of EMF for base stations using signal decoding technique," in *Proc. URSI Asia–Pacific Radio Sci. Conf. (AP-RASC)*, Mar. 2019, pp. 179–183.
[28] Y. S. Lee, S. B. Jeon, A.-K. Lee, K. Kim, J.-K. Pack, and H.-D. Choi, "Study on the appropriate measurement spacing for EMF installation compliance assessments of a 3.5 GHz 5G base station," *IEEE Access*, vol. 9, pp. 88167–88176, 2021.
[29] *Determination of RF Field Strength, Power Density and SAR in the Vicinity of Radiocommunication Base Stations for the Purpose of Evaluating Human Exposure*, Standard IEC 62232, Committee Draft, Ed. 3.0, Jun. 2020.
[30] International Commission on Non-Ionizing Radiation Protection, "Guidelines for limiting exposure to time-varying electric, magnetic, and electromagnetic fields (up to 300 GHz)," *Health Phys.*, vol. 118, no. 5, pp. 483–524, May 2020.
[31] T. J. Walters, D. W. Blick, L. R. Johnson, E. R. Adair, and K. R. Foster, "Heating and pain sensation produced in human skin by millimeter waves: Comparison to a simple thermal model," *Health Phys.*, vol. 78, no. 3, pp. 259–267, Mar. 2000.
[32] K. H. Joyner, C. C. Davis, E. C. Elson, E. M. Czerska, and P. Czerski, "An automated dosimetry system for microwave and thermal exposure of biological samples *in vitro*," *Health Phys.*, vol. 56, no. 3, pp. 303–307, Mar. 1989.
[33] F. V. Van Breugel, J. N. Kutz, and B. W. Brunton, "Numerical differentiation of noisy data: A unifying multi-objective optimization framework," *IEEE Access*, vol. 8, pp. 196865–196877, 2020.
[34] K. R. Foster, M. C. Ziskin, Q. Balzano, and A. Hirata, "Thermal analysis of averaging times in radio-frequency exposure limits above 1 GHz," *IEEE Access*, vol. 6, pp. 74536–74546, 2018.

YOUNG SEUNG LEE (Member, IEEE) received the B.S. degree in radio communications engineering from Korea University, Seoul, Republic of Korea, in 2006, and the M.S. and Ph.D. degrees in electrical engineering from the Korea Advanced Institute of Science and Technology, Daejeon, Republic of Korea, in 2008 and 2012, respectively. Since 2012, he has been with the Electronics and Telecommunications Research Institute, Daejeon, where he is currently a Principal Researcher. His current research interests include exposure system design, compliance assessment, and numerical dosimetry with an emphasis on 5G frequencies. He is also concerned with electromagnetic theory, antenna propagation, and measurement.

SANG BONG JEON received the B.S., M.S., and Ph.D. degrees in electronic engineering from Yeungnam University, Gyeongsan, Republic of Korea, in 2001, 2003, and 2007, respectively. From 2008 to 2010, he was a Senior Research Engineer at the Korea Radio Promotion Association, Seoul, Republic of Korea, where he conducted research in the fields of electromagnetic compatibility technology. Since 2010, he has been with the Radio and Satellite Research Division, Electronics and Telecommunications Research Institute, Daejeon, Republic of Korea. His research interests include bio-electromagnetics and electromagnetic compatibility.

JEONG-KI PACK received the B.S. degree in electronic engineering from Seoul National University, Seoul, South Korea, in 1978, and the M.S. and Ph.D. degrees in electromagnetic wave propagation from Virginia Tech, Blacksburg, VA, USA, in 1985 and 1988, respectively. From 1978 to 1983, he worked at the Agency for Defense Development, South Korea, as a Researcher. In 1988, he joined ETRI and moved to Dong-A University, in 1989. Since February 1995, he has been with the Department of Radio Science and Engineering, Chungnam National University, Daejeon, South Korea, as a Professor, where he is currently an Emeritus Professor. His research interests include electromagnetic wave propagation and bio-electromagnetics.

NAM KIM received the B.S., M.S., and Ph.D. degrees in electronics engineering from Yonsei University, Seoul, South Korea, in 1981, 1983, and 1988, respectively. He has been a Professor with the School of Information and Communication Engineering, Chungbuk National University, Cheongju, South Korea, since 1989. His research interests include optical information processing, health effect of the EMF, wireless power transfer, and antennas for mobile communications. He is a member of the International Advisory Committee for the World Health Organization Project on EMF, the IEEE International Committee on Electromagnetic Safety, and the International Electro Technical Commission TC 106. He was the President of the Bioelectromagnetics Society.

HYUNG-DO CHOI received the M.S. and Ph.D. degrees in material sciences from Korea University, Seoul, Republic of Korea, in 1989 and 1996, respectively. Since 1997, he has been with the Electronics and Telecommunications Research Institute, Daejeon, Republic of Korea, where he is currently a Project Leader of the Radio and Satellite Research Division. His research interests include biological effects of RF radiation and developed RF radiation protection standards.